

Single-cell Characterization of Autotransporter-mediated *Escherichia coli* Surface Display of Disulfide Bond-containing Proteins^{*[S]}

Received for publication, June 4, 2012, and in revised form, September 24, 2012. Published, JBC Papers in Press, September 27, 2012, DOI 10.1074/jbc.M112.388199

Balakrishnan Ramesh[‡], Victor G Sendra[‡], Patrick C Cirino[‡], and Navin Varadarajan^{‡S1}

From the Departments of [‡]Chemical and Biomolecular Engineering and ^SBiomedical Engineering, University of Houston, Houston, Texas 77204

Background: The ability of autotransporter (AT) to translocate polypeptides with multiple disulfide bonds is controversial.

Results: Surface display of functional chymotrypsin (4 S-S) and M18 scFv (2 S-S) was quantitatively characterized.

Conclusion: Surface display of functional recombinant protein with multiple disulfide bonds can be achieved using AT system.

Significance: Displaying recombinant proteins with disulfide bonds enhances utility of ATs.

Autotransporters (ATs) are a family of bacterial proteins containing a C-terminal β -barrel-forming domain that facilitates the translocation of N-terminal passenger domain whose functions range from adhesion to proteolysis. Genetic replacement of the native passenger domain with heterologous proteins is an attractive strategy not only for applications such as biocatalysis, live-cell vaccines, and protein engineering but also for gaining mechanistic insights toward understanding AT translocation. The ability of ATs to efficiently display functional recombinant proteins containing multiple disulfides has remained largely controversial. By employing high-throughput single-cell flow cytometry, we have systematically investigated the ability of the *Escherichia coli* AT Antigen 43 (Ag43) to display two different recombinant reporter proteins, a single-chain antibody (M18 scFv) that contains two disulfides and chymotrypsin that contains four disulfides, by varying the signal peptide and deleting the different domains of the native protein. Our results indicate that only the C-terminal β -barrel and the threaded α -helix are essential for efficient surface display of functional recombinant proteins containing multiple disulfides. These results imply that there are no inherent constraints for functional translocation and display of disulfide bond-containing proteins mediated by the AT system and should open new avenues for protein display and engineering.

The display of recombinant proteins on the surface of microorganisms has attracted substantial interest from both an application (biotechnological or clinical) and a basic microbiological standpoint toward understanding mechanisms of protein translocation. The utility of surface display of functional peptides and proteins for biotechnological applications has been demonstrated in several different contexts including: whole-cell biocatalysis based on esterases (1), bioremediation using recombinant display of organophosphorous hydrolases and

metallothioneins (2, 3), glucose-responsive biosensors (4), and protein engineering of displayed libraries (5, 6). In the context of surface display of antigenic recombinant peptides/proteins for delivery of live vaccines, besides the obvious safety advantage of using surface display on nonpathogenic bacteria, there are several other benefits such as the cost and ease of manufacturing, the ability of bacterial components such as lipopolysaccharide (LPS) to function as adjuvants to stimulate the immune system via Toll-like receptors leading to sustained immunity (7), and the ability of the mammalian innate immune system to recognize prokaryotic mRNA (present only in live cells) leading to protective immunity (8).

In parallel, surface display of both recombinant and engineered native proteins has been used to delineate the mechanism of protein translocation. In Gram-negative bacteria such as *Escherichia coli* in particular, display of proteins on the cell surface requires that the protein that is translated in the cytoplasm traverse across two separate lipid bilayers, the inner and outer membranes (9). Consequently, Gram-negative bacteria have evolved a diverse array of protein transport machinery (designated types I–VIII) dedicated to facilitating the translocation and ultimately secretion or surface display of proteins (10). Autotransporters (ATs,² type Va) are believed to be the most abundant secretion pathway with >700 members that are ubiquitous in bacterial genomes (11, 12).

ATs comprise an extended N-terminal leader sequence that is cleaved at the inner membrane (13) followed by an N-terminal passenger (20–400 kDa) typically associated with virulence functions (adhesion, proteolysis, pore formation, etc.) and finally a conserved C-terminal \sim 30-kDa β -barrel (14). ATs are attractive candidates for the surface display of recombinant proteins because they are displayed at high-copy numbers (>100,000 protein copies) with minimal host toxicity (15). The nomenclature of ATs was based on the assumption that the primary sequence of the protein encodes all the information necessary for accurate translocation and ultimately surface dis-

* This work was supported by the Welch Foundation (Grant E-1774) and University of Houston Startup funds.

[S] This article contains supplemental Tables S1 and S2 and Figs. S1–S7.

¹ To whom correspondence should be addressed. Tel.: 713-743-1691; Fax: 713-743-4323; E-mail: nvaradar@central.uh.edu.

² The abbreviations used are: AT, autotransporter; Ag43, Antigen 43; ChyB, chymotrypsin; rChyB, recombinant chymotrypsin; PE, phycoerythrin; BME, β -mercaptoethanol; OmpT, outer membrane protease T; aa, amino acid(s); rPAD4, recombinant PAD4; Hbp, hemoglobin-binding protease.

play or secretion of the passenger domain. Although it was initially hypothesized that the C-terminal β -barrel formed a pore through which the N-terminal passenger was translocated (16), this model has subsequently been challenged, and an alternative model based on the aid of accessory proteins such as the Bam complex has been developed (17, 18). Recent biochemical and functional studies on the C-terminal domain indicated that a conserved α -helix and the β -barrel comprise the minimum functional transport unit (19), but the role of the α -helix has since been suggested to be required for cleavage rather than actual secretion (20).

There exists considerable controversy in the ability of ATs to transport passengers, either native or recombinant, containing folded elements, especially those containing disulfide bonds. Since disulfide bond formation is catalyzed in the periplasm of *E. coli* by the Dsb family of oxidoreductases, proteins containing thiols that form disulfide bonds are expected to be oxidized in the periplasm (21). Using both native (EspP, IcsA) and recombinant (single chains of antibodies) passengers, several groups have independently reported the ability of the passenger domain to fold in the periplasm in a proteolytically resistant state and subsequently be transported across the outer membrane (22–26). In contrast, studies utilizing native passengers engineered to contain cysteine residues (Hbp, plasmid-encoded toxin (Pet)) have indicated that to a large extent, disulfide bonds between cysteines that are not closely spaced stall passenger transport (27–29).

An understanding of the variations in functional protein display at a single-cell level and quantifying the frequencies of cells in a clonal population capable of expressing functional protein can provide insight into constraints imposed by the folded state of passenger on its transport. At the same time, quantifying the ability of ATs to display recombinant antigenic proteins containing multiple disulfide bonds would facilitate the adaptation of ATs for live-cell vaccine applications. Similarly, biotechnological applications that involve displaying libraries of protein molecules require knowledge of the number of functional recombinant protein molecules displayed on every single cell. Although flow cytometry has been previously applied to study of ATs, these have been predominantly restricted to quantifying epitope tags that indicate surface protein display and not functional protein display (7, 19, 30).

Here, we systematically investigate the ability of Antigen 43 (Ag43) to display two different recombinant reporter proteins that are known to fold in the periplasm, a single-chain antibody (scFv), which contains two disulfides, and recombinant chymotrypsin (rChyB), which contains four disulfides (31, 32). Using flow cytometry to quantify surface display of functional protein at the single-cell level, we demonstrate that despite the known propensity of these passengers to fold in the periplasm, surface display of these proteins is rather efficient and can be achieved using only the C-terminal domain containing the α -helix and the β -barrel. Our flow cytometric data are consistent with data obtained by immunofluorescence microscopy and Western blotting on whole-cell lysates. In contrast to previous studies (33), no genetic manipulation such as the use of dsbA⁻ strains or the use of reducing agents such as β -mercaptoethanol (BME) was necessary to accomplish efficient display. Our results indi-

cate that display of recombinant proteins containing multiple disulfides can be achieved by employing the Ag43 system and that the vast majority of native ATs including the autochaperone domain are not indispensable for heterologous protein display. These results have important implications for understanding both the protein translocation by ATs and the recombinant display of heterologous proteins for catalysis and engineering.

EXPERIMENTAL PROCEDURES

Plasmid Construction—Gene fragments coding for recombinant passenger (M18 scFv and *Rattus norvegicus* chymotrypsin (ChyB)) and signal peptides of Ag43, outer membrane protease T (OmpT), and pectate lyase (PelB) were obtained by PCR using oligonucleotides (Integrated DNA Technologies), as listed in supplemental Table S1. Templates for PCR to obtain gene fragments coding for M18 scFv and rChyB were kind gifts from the laboratory of G. Georgiou (University of Texas, Austin, TX). Genomic DNA of *E. coli* MC1061 was used as template to obtain other gene fragments. *E. coli* MGB263 was a kind gift from Dr. Marcia Goldberg (Harvard School of Public Health, Boston, MA). The genes coding for fragments of Ag43 (138–1039, 552–1039, and 700–1039 amino acids (aa)) were amplified by PCR with oligonucleotides designed to encode a (GGGGS)₂ linker (5') and His₆ tag, in addition to restriction enzyme recognition sites (3') (supplemental Table S1). The PCR product was subsequently digested with KpnI and HindIII at 37 °C for 3 h and was ligated using T4 DNA ligase at 25 °C for 4 h to pBAD33 cut using the same restriction enzymes. The ligated plasmids were then transformed into competent *E. coli* MC1061 via electroporation and verified by standard Sanger sequencing. This family of vectors designated pBAD_138, pBAD_552, and pBAD_700 containing the C-terminal fragments from Ag43 was used for the easy cloning of different passenger/leader combinations. The genetic fusion of signal peptide to 5' region of recombinant passenger gene was accomplished via the use of complementary oligonucleotides (supplemental Table S1) by overlap extension PCR, essentially as described previously (34). Following overlap extension PCR, the product was gel-purified, digested with SacI and KpnI at 37 °C for 3 h, and ligated into the appropriate plasmid constructs. Ligated plasmids were transformed in to *E. coli* MC1061 cells (34) by electroporation and verified by standard Sanger sequencing. All plasmids use a standardized nomenclature (see Table 1) that indicates the leader, the passenger, and the residues that originate from AT. For example, plasmid pBAD_AM18_138 contains the gene encoding for a fusion protein that has signal peptide of Ag43, M18 scFv, and 138–1039 aa of Ag43 AT.

Expression and Labeling of M18 scFv—A standard 3-ml culture of cells harboring plasmids to surface display M18 scFv (e.g. pBAD_M18_138) was grown in LB medium (BD Diagnostics) in the presence of 30 μ g/ml chloramphenicol (Thermo Fisher Scientific) to an optical density (A_{600}) of 0.6 at 25 °C. Cells were then induced via the addition of 0.2% L-arabinose (Sigma) to express M18 scFv for 12 h at 25 °C. The presence of M18 scFv on the surface of *E. coli* was characterized by the ability of intact cells to bind antigens (PA₆₃ and PAD4) using flow cytometry.

AT-mediated Display of Proteins with Disulfide Bonds

PAD4 containing FLAG epitope tag (rPAD4) was recombinantly expressed in *E. coli* and purified as described previously (35), and PA₆₃-FITC was obtained from List Biological Laboratories, Inc. 100 μ l of cells expressing M18 scFv from the appropriate construct normalized to A₆₀₀ of 2 units were washed twice in PBS and incubated with 200 nM rPAD4 for 1 h at 25 °C. Cells were then washed, resuspended in 20 μ l of PBS, and incubated with 40 nM anti-FLAG-phycoerythrin (PE) (ProZyme, Inc.) at 25 °C for 45 min in the dark. For labeling using PA₆₃, 25 μ l of cells at A₆₀₀ = 2 were washed twice in PBS and incubated with 300 nM PA₆₃-FITC at 25 °C for 1 h in the dark. A 5- μ l aliquot of cells labeled with fluorophore was diluted with 0.5 ml of PBS and analyzed by flow cytometry.

Expression and Labeling of rChyB—Cells harboring pBAD_AChy_700 (Table 1) were grown in 3 ml of LB medium supplemented with 30 μ g/ml chloramphenicol to A₆₀₀ = 0.6 at 37 °C. Protein expression was induced at 37 °C for 2 h using 0.2% L-arabinose. To characterize the proteolytic activity of chymotrypsin, a peptide substrate (Chy-BQ7) was obtained by conjugating the synthetic peptide (Ac-CAAPYGSKGRGR-CONH₂) (GenScript) to a fluorophore (BODIPY) (Invitrogen) and a nonfluorescent quencher (QSY7) (Invitrogen) as described previously (36) (supplemental Fig. S6). 1 ml of cells at A₆₀₀ = 0.1 were washed twice in 1% sucrose (Sigma) solution and incubated for 1 h with 20 nM Chy-BQ7 at 25 °C in the dark. Surface display of chymotrypsin was independently verified by incubating whole cells with an antibody that can bind to chain C of rChyB (Santa Cruz Biotechnology, Inc.). 20 μ l of cells expressing chymotrypsin at A₆₀₀ = 2 were washed twice in PBS and incubated with 50 μ g/ml biotin-conjugated anti-chyB antibody for 1 h. Cells were subsequently washed with PBS and incubated with 5 μ g/ml streptavidin-conjugated PE (Jackson ImmunoResearch) for 30 min at 25 °C in the dark. A 5- μ l aliquot of cells labeled with fluorophore was diluted with 0.5 ml of PBS or 1% sucrose and analyzed by flow cytometry.

Flow Cytometry—Cells labeled with fluorophore were analyzed using the BD FACSJazz cell sorter (BD Biosciences) at ~8000 events/second and offset of 1. For all samples, a minimum of 10,000 events was recorded, and the events were triggered using side scatter. Fluorophores were excited using a 488-nm laser, and emission was measured using 530/40 (BODIPY and FITC) and 580/30 (PE) filters.

Immunofluorescence Microscopy—Cells expressing chymotrypsin were labeled using biotinylated antibody against chain C of chymotrypsin (Santa Cruz Biotechnology) and PE conjugated to streptavidin as described above. After washing with PBS to remove excess fluorophore, cells were resuspended to an A₆₀₀ = 1. Slide preparation was performed as described previously (53). Briefly, 2 μ l of cell suspension was pipetted on a glass slide, and a small piece of agarose pad was placed on top of it to prevent cell movement. Microscopy was performed using an inverted epifluorescence microscope (Eclipse Ti, Nikon) with a 100 \times objective (Plan Fluor, NA 1.4, oil immersion) and Cy3 filter cube (Nikon). Images were captured in a cooled 1024 \times 1024 EMCCD camera (Cascade II 1024, Photometrics) at a gain of 2000 and an exposure time of 100 ms using Nikon Elements software (Nikon).

Western Blotting—A standard 3-ml culture of cells displaying recombinant protein (M18 scFv or rChyB) was obtained as described above. A whole-cell pellet obtained by centrifugation at 16,000 \times g for 2 min was resuspended in 2 \times sample buffer (Bio-Rad) diluted with equal volume of 50 mM Tris (Sigma) and boiled at 100 °C for 5 min. SDS-PAGE of samples (10⁷ cells/lane) was performed at 120 V for 90 min in a 4–12% polyacrylamide gel (Lonza) using a Mini-PROTEAN gel electrophoresis system (Bio-Rad). After electrophoresis, protein molecules were transferred to a PVDF membrane (Bio-Rad) at 100 V for 60 min using a wet electroblotting system (Bio-Rad). Procedures for SDS-PAGE and blotting were adapted from Ref. 37. To reduce nonspecific binding, the membrane was blocked by overnight treatment with Tris-buffered saline containing 5% milk and 0.1% Tween 20 (Bio-Rad). Membrane was labeled using rabbit anti-His antibody (300 ng/ml, GenScript), goat anti-rabbit antibody conjugated to HRP (40 ng/ml, Jackson ImmunoResearch), and chemiluminescent HRP substrate (SuperSignal West Pico, Thermo Scientific). Protein marker (15–225 kDa, EMD Millipore) was used as reference in estimating the size of bands. Chemiluminescent imaging of developed blot was performed using a CCD camera in an imaging cabinet (Alpha Innotech Fluorchem SP).

RESULTS

Surface Display of Functional Single-chain Antibody via Fusion to Ag43 Revealed by Flow Cytometry—Ag43, a native *E. coli* AT, mediates bacterial autoaggregation via self-recognition of the passenger domains (38). It is synthesized as a 1039-aa polypeptide containing the following domains: a leader peptide (aa 1–52); an N-terminal unstructured domain of unknown function (aa 53–138); a passenger with a β -helical core (aa 138–552) containing a proteolytic site (551–552) and a putative autochaperone domain (aa 600–707); and an α -helix (aa 710–730) that is threaded via the C-terminal β -barrel pore (aa 731–1039) (Fig. 1A). The domains were identified by homology modeling of Ag43 using PHYRE server (39). To investigate the ability of the AT to mediate display of recombinant proteins containing disulfides, we synthesized a genetic construct coding for the native Ag43 leader, single-chain antibody (scFv) M18, and aa 138–1039 from Ag43 via standard overlap extension PCR in a two-step cloning strategy.

The M18 scFv contains two disulfides, one in each of the variable regions, and is an ~25-kDa globular protein. It was previously isolated using bacterial display as a high-affinity (K_d = 35 pM) binder to anthrax toxin protective antigen (31). The functional status of M18 scFv when displayed as a fusion to Ag43 was investigated using flow cytometry. Protein expression was induced from pBAD_AM18_138 using L-arabinose for 12 h, and the cells were incubated with FITC-labeled heptameric PA₆₃. Flow cytometry revealed that cells expressing M18 scFv were bimodal (Table S2, Fig. 2A, 30% positive, mean = 83), whereas cells surface displaying an irrelevant protein or uninduced cultures were uniformly negative (Fig. 2A, mean = 3). To ensure that our single-cell functional assay only detects folded disulfide bond-containing proteins, a cysteine-free M18 scFv variant (AM18_C/A_700) was synthesized by standard overlap

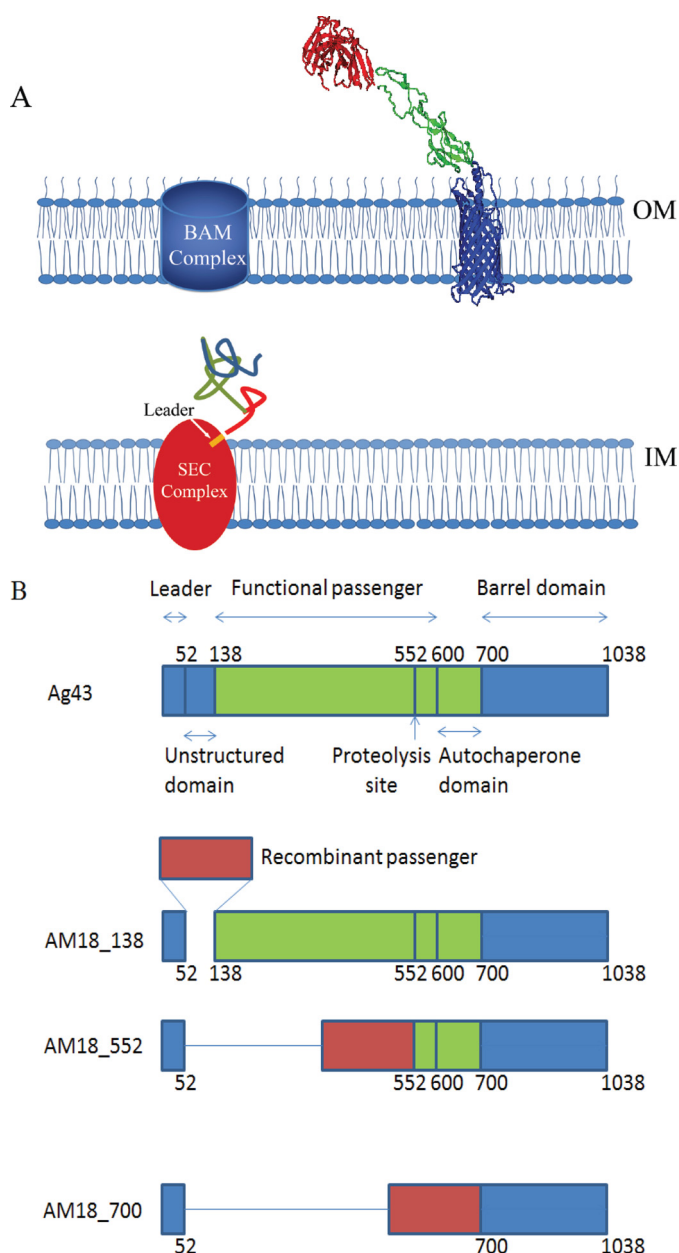


FIGURE 1. AT mediated display of recombinant proteins. *A*, schematic describing the transport of AT to the outer membrane. AT polypeptides synthesized in the cytoplasm are targeted by its leader peptide to the Sec complex, which is responsible for translocation of proteins across the inner membrane (*IM*). During the transport across the inner membrane, the leader peptide is cleaved from rest of the AT polypeptide by proteolysis. Formation of disulfide bonds catalyzed by dsbA can occur in the periplasm. β -Barrel assembly machinery (*BAM*) complex interacts with the barrel domain of AT to facilitate its translocation across the outer membrane (*OM*). After translocation, functional passenger domain can remain surface-bound or be secreted into the extracellular environment. *B*, schematic of Ag43 and fusion proteins containing recombinant passenger (red), Ag43 passenger (green), and Ag43 barrel domain (blue) used in this study. Positions (aa numbering based on Ag43) of various domains identified by homology modeling of Ag43 are shown.

PCR. As expected, cells expressing AM18_C/A_700 showed poor labeling with PA63-FITC (supplemental Fig. S1, 2% positive, mean = 28). Similarly, to establish the requirement of the AT for surface display, cells expressing the soluble form of M18 (PM18) were labeled and shown to be negative (supplemental Fig. S1).

In parallel, Western blotting experiments were performed with whole-cell lysates to confirm the presence of the fusion construct. Recombinant fusion protein expressed from pBAD_AM18_138 was immunoblotted using a rabbit anti-His antibody (Fig. 2*B*). In addition to the full-length protein (135 kDa), additional bands corresponding to degraded protein were observed (35 kDa), consistent with the prolonged induction.

C-terminal Domains Comprising the β -Barrel and the α -Helix Are Sufficient to Achieve Efficient Surface Display—Because initial studies utilizing cells harboring pBAD_AM18_138 indicated that functional surface display of M18 scFv could be achieved, we next sought to systematically investigate the contribution of the different domains of Ag43 to the surface display of M18 scFv. Accordingly, two separate plasmids designated pBAD_AM18_552 and pBAD_AM18_700 (Fig. 1*B*) were constructed using site-overlap extension. pBAD_AM18_552 encodes a truncated N-terminal passenger but an intact autochaperone domain, whereas pBAD_AM18_700 does not encode the autochaperone domain (Fig. 1*B* and Table 1).

Protein expression was induced by the addition of L-arabinose for 12 h, and the cells were labeled using PA₆₃-FITC and analyzed on the flow cytometer. Cells expressing pBAD_AM18_552 were reproducibly less efficient (Fig. 2*A*, 9% positive, mean = 40) at functional M18 scFv display when compared with pBAD_AM18_138. In contrast, greater than half of all cells harboring pBAD_AM18_700 showed expression of M18 scFv on the surface (Fig. 2*A*, 56% positive, mean = 75), demonstrating that at least for recombinant expression of M18 scFv, the C-terminal domains containing the α -helix and β -barrel are sufficient.

Binding of Bulky Antigens Is Not Sterically Hindered—The ability of the carbohydrate chains of lipopolysaccharide (LPS) to interfere with protein labeling on the cell surface is well documented (41). Because our labeling strategy utilized the large heptameric antigen PA₆₃ to probe the functional status of M18 scFv, we tested whether steric hindrance from LPS could explain the heterogeneity of the population in the efficiency of surface display. The epitope of M18 scFv has been mapped to domain 4 within protective antigen (PAD4), and the construction, expression, and purification of recombinant PAD4 (rPAD4) with an N-terminal FLAG epitope tag (DYKDDDDK) have been reported previously (42). Cells expressing pBAD_AM18_700 were incubated first with rPAD4 (200 nM) and then with anti-FLAG-PE (40 nM) and interrogated on the flow cytometer. Based on comparison of frequency of cell population that can bind to rPAD4 (46% positive) and PA₆₃-FITC (51% positive), we can infer that binding of M18 scFv to its antigen does not appear to be sterically hindered with this expression system (Fig. 3).

The Extended Signal Peptide Region Is Not Indispensable for Functional Surface Display—Signal peptides are responsible for translocation of AT across the inner membrane. In contrast to other periplasmic proteins or even other outer membrane proteins, the signal peptides of AT have an extended N-terminal region, and it has been previously hypothesized that the extended N-terminal region prevents the passenger domain from acquiring a conformation incompetent for translocation (13). To quantitatively determine the significance of the

AT-mediated Display of Proteins with Disulfide Bonds

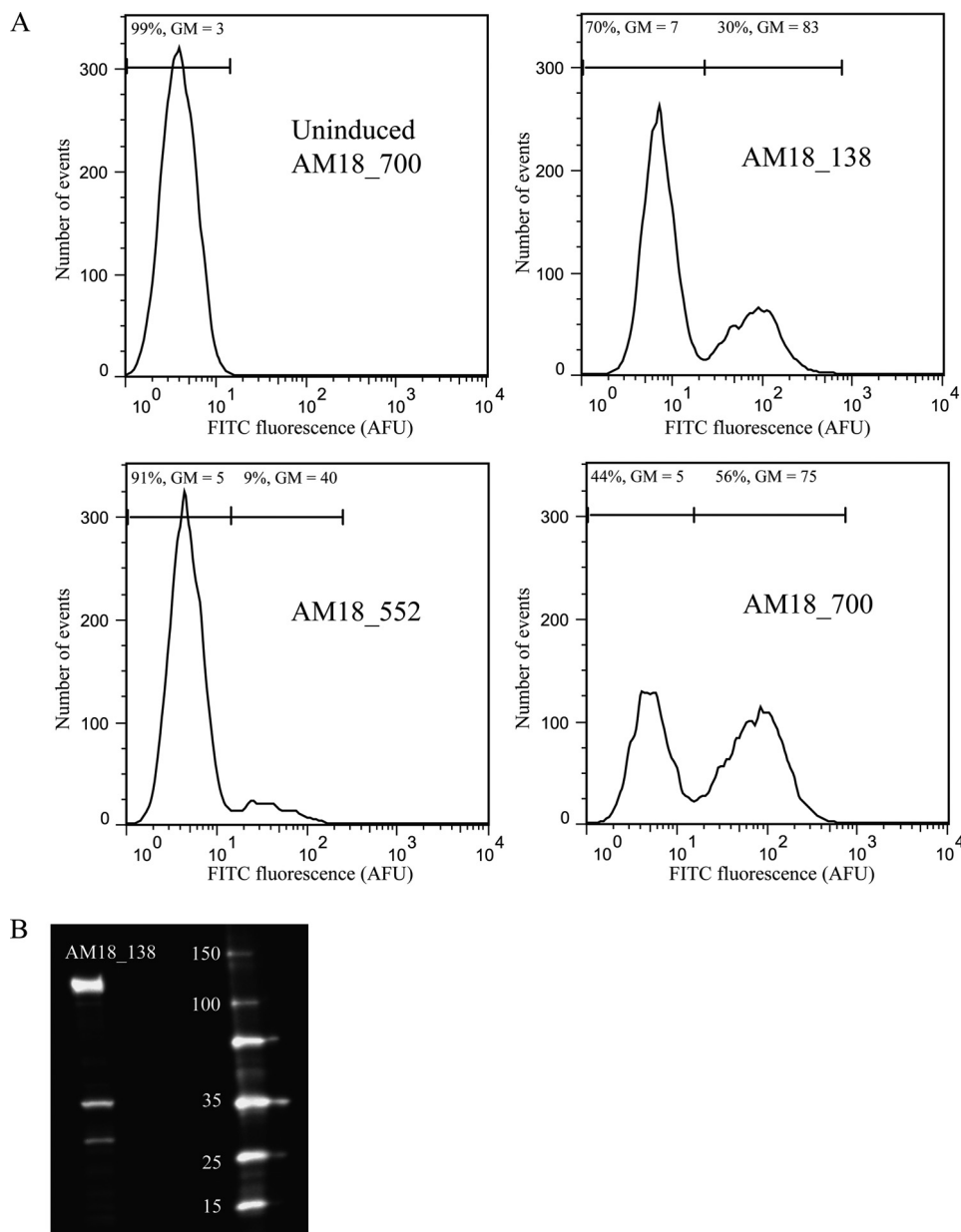


FIGURE 2. Surface expression of functional M18 scFv as a function of native passenger length. *A*, flow cytometric quantification of AT-mediated display by fusion of M18 scFv to: (i) 138–1039 aa of Ag43 containing a majority of the native passenger, (ii) 552–1039 aa containing N-terminally truncated native passenger but an intact autochaperone domain, and (iii) 700–1039 aa containing the α -helix and β -barrel. *E. coli* MC1061 cells expressing M18 scFv were labeled using PA₆₃-FITC. Uninduced cells containing pBAD_AM18_700 were used as negative control. *AFU*, arbitrary fluorescence units. *B*, Western blot showing the presence of AM18_138 (expected size in the absence of autoproteolysis = 135 kDa). Uninduced cells harboring pBAD_AM18_138 was used as negative control. Blot was developed using rabbit anti-His antibody (300 ng/ml), goat anti-rabbit antibody conjugated to HRP (40 ng/ml), and chemiluminescent HRP substrate.

TABLE 1

List of plasmids used in this study

pBAD33 was used as the cloning vector and contains chloramphenicol resistance marker.

Plasmid	Leader	Recombinant passenger	aa from Ag43 AT
pBAD_AM18_138	Ag43	M18 scFv	138–1039 aa
pBAD_AM18_552	Ag43	M18 scFv	552–1039 aa
pBAD_AM18_700	Ag43	M18 scFv	700–1039 aa
pBAD_OM18_700	OmpT	M18 scFv	700–1039 aa
pBAD_PM18_700	PelB	M18 scFv	700–1039 aa
pBAD_AChy_700	Ag43	34–263 aa of rat chymotrypsin	700–1039 aa
pBAD_AM18_C/A_700	Ag43	M18 scFv with C28A, C93A, C155A, and C229A mutations	700–1039 aa
pBAD_PM18	PelB	M18 scFv	Soluble expression, no fusion to Ag43

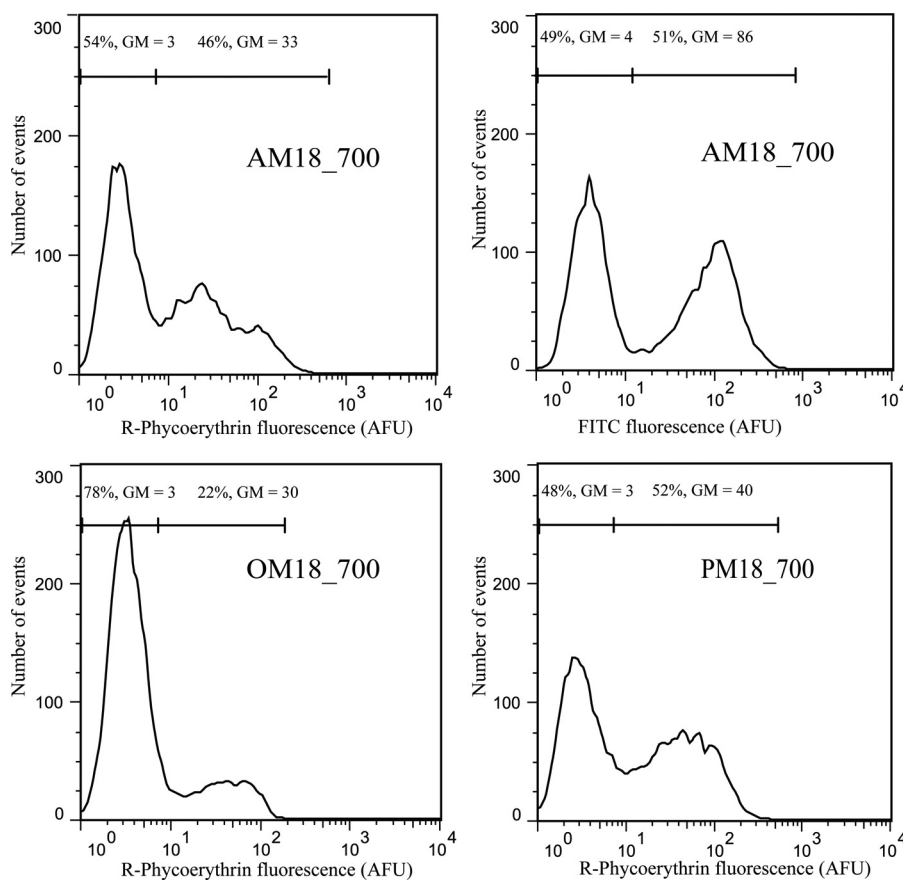


FIGURE 3. **Surface expression of functional M18 as a function of N-terminal leader sequence.** Flow cytometric quantification of AT-mediated display using leader sequences of PelB, a periplasmic protein, and OmpT, an outer membrane protein, was performed. *E. coli* MC1061 cells expressing M18 scFv were labeled with rPAD4 and anti-FLAG-PE and analyzed using flow cytometry. Functional M18 expressed on the surface can also bind to bulky antigen. Cells displaying M18 expressed from pBAD_AM18_700 were labeled with PA₆₃-FITC (heptamer) and analyzed using flow cytometry. AFU, arbitrary fluorescence units.

extended native signal peptide at the single-cell level, two additional fusion constructs were synthesized by PCR and cloned into pBAD33. Because our data indicated that efficient surface display is accomplished via fusion to the C-terminal domains of Ag43 (700–1039 aa) (Fig. 2A), these were used as optimal fusion partners. pBAD_PM18_700 encodes for a tripartite fusion between the leader sequence of pectate lyase B (PelB), a periplasmic protein, M18 scFv and Ag43 (residues 700–1039), and pBAD_OM18_700 for an identical tripartite fusion with the leader sequence of OmpT, an outer membrane protein (Table 1). Flow cytometric analysis of M18 scFv using rPAD4 immunofluorescent sandwiches (Fig. 3) demonstrated that the frequency of cells harboring pBAD_AM18_700 (native leader, 46% positive) was not largely different from those harboring pBAD_PM18_700 (PelB leader, 52% positive). However, populations of cells expressing pBAD_OM18_700 (OmpT leader, 22% positive) were not as efficient in the functional display of M18 scFv. These results indicate that although the native Ag43 leader is not a requirement for AT-mediated surface display, substituting the leader sequence from other outer membrane proteins such as OmpT leads to suboptimal display of functional protein molecules on the surface (Fig. 3).

Surface Display of Functional M18 scFv Is Not Improved by the Addition of Reducing Agents or the Use of Protease-deficient Strains—Prior work has demonstrated that the surface display of disulfide bond-containing passengers using the AT system is

hampered by the formation of disulfide bonds in the periplasm and that the yield of surface displayed protein can be improved either by the use of genetically engineered *E. coli* strains (*dsbA*⁻) or by the addition of reducing agents such as BME during cell growth and protein expression (26, 43, 44). To test this hypothesis in the current context, cells expressing pBAD_AM18_700 were grown to mid-log phase, and expression of M18 scFv was induced for 12 h in LB medium containing 10 mM BME. Subsequently, the cells were transferred to media devoid of BME for 1 h to facilitate refolding prior to analysis. An aliquot of cells was incubated with rPAD4 and anti-FLAG-PE, and the populations were analyzed on the flow cytometer. Growth and induction in the presence of BME had a negative effect on functional M18 scFv display (10% positive, mean = 13) when compared with an identical culture grown without BME (36% positive, mean = 38) (supplemental Fig. S2). Secondly, to test whether the use of OmpT knock-out strains would improve the frequency of cells expressing functional M18 scFv, we used the isogenic *E. coli* MGB263 as the host for surface display. Flow cytometric analysis of cells expressing pBAD_AM18_700 revealed that both the frequency and the mean of cells expressing functional M18 scFv were identical in both strains (supplemental Fig. S3), indicating that OmpT-mediated proteolysis had no discernible effect on functional protein display in our current system.

AT-mediated Display of Proteins with Disulfide Bonds

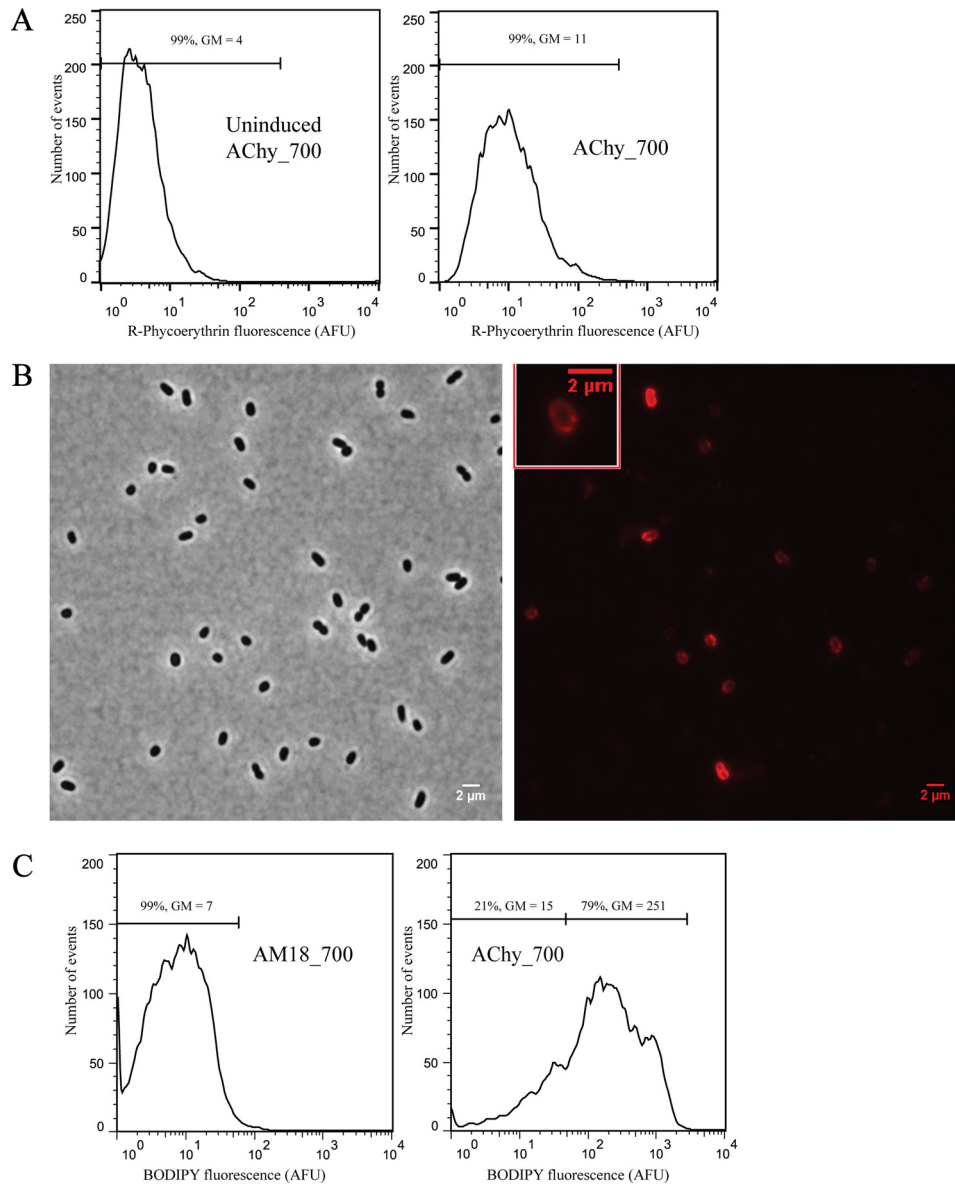


FIGURE 4. Functional chymotrypsin displayed on the surface of *E. coli* via fusion to Ag43. *A*, flow cytometry analysis of cells expressing rChyB labeled with biotin-conjugated anti-ChyB antibody (chain C-specific) and streptavidin-PE. *B*, immunofluorescence microscopy showing surface display of chymotrypsin. Cells harboring pBAD_AChy_700 were induced with 0.2% L-arabinose and labeled with biotin-conjugated anti-ChyB antibody (chain C-specific) and streptavidin-PE. An enlarged image of a cell is shown in the *inset*. A corresponding image obtained in phase contrast mode is also shown. *C*, flow cytometry analysis of cells expressing rChyB labeled with Chy-BQ7 FRET substrate containing a chymotrypsin-sensitive linker. *AFU*, arbitrary fluorescence units.

Surface Display of Chymotrypsin—*R. norvegicus* chymotrypsin B (*chyB*) is a prototypical serine protease that cleaves immediately after amino acids with aromatic side chains such as tyrosine. ChyB has three chains (A, B, and C) held together by disulfide bonds, and mature rChyB containing only chains B and C (aa 34–263) contains the peptidase unit and is catalytically active. rChyB contains four disulfide linkages (aa 60–76, 154–219, 186–200, and 209–238, chymotrypsinogen numbering) and folds into a globular structure that is very different from the standard β -solenoid-like folds of AT passengers.

To investigate the ability of Ag43 to display rChyB on the cell surface, a genetic fusion with both *ag43* leader and the gene coding for C-terminal domains (aa 700–1039) of Ag43 was constructed using PCR and cloned into pBAD33 to yield pBAD_AChy_700 (Table 1). Because chymotrypsin nonspecifically

degrades cellular proteins, we rationalized that lower protein expression would preserve cell viability. Secondly, because chymotrypsin is an enzyme, we reasoned that we could detect lower levels of expressed protein using a catalytic assay in comparison with the antibody-based stoichiometric assay. Cells containing pBAD_AChy_700 were therefore induced at 37 °C for only 2 h. Cells were subsequently labeled with biotin-conjugated anti-ChyB antibody (chain C-specific) and streptavidin-PE and analyzed on the flow cytometer. Cells expressing pBAD_AChy_700 (mean = 11) were uniformly labeled and could be reproducibly detected (Fig. 4*A*) when compared with either uninduced or M18 scFv-expressing cells (mean = 4), confirming the surface display of rChyB using the AT system. Expression levels were lower, as anticipated by the brief period of protein expression. The pres-

ence of full-length fusion protein was also independently confirmed by immunoblotting employing an anti-His antibody (supplemental Fig. S4).

Next, we evaluated the surface localization of the recombinant chymotrypsin molecules using immunofluorescent microscopy. *E. coli* cells expressing rChyB were detected using a biotinylated antibody specific for chain C. Consistent with our flow cytometry data, pBAD_AChy_700 displayed uniform expression on both the polar and the lateral surfaces (Fig. 4B). No fluorescence was observed when either uninduced cells or cells expressing pBAD_AM18_138 were labeled under identical conditions (supplemental Fig. S5).

Examination of the morphology of cells expressing AChy_700 indicated that the cells were coccoid. We confirmed that the coccoid nature was an experimental artifact due to the extended time required for labeling and subsequent imaging (~3 h) of live cells and not due to protein expression (supplemental Fig. S5).

rChyB Displayed on the Surface Is Enzymatically Active—The enzymatic activity of surface-displayed rChyB was investigated using a Förster resonance energy transfer (FRET)-based peptide assay on the flow cytometer, essentially as described previously (36). Briefly, cells displaying the protease are incubated with a positively charged peptide substrate that contains a protease-sensitive linker sandwiched between a FRET pair. Cleavage of the peptide linker leads to loss of FRET, and the product molecules are captured locally on the same cells using electrostatic interactions (supplemental Fig. S6). Cells expressing pBAD_AChy_700 were incubated with 20 nM of the ChyBQ7 FRET substrate containing a chymotrypsin-sensitive linker for 1 h in 1% sucrose. Subsequent flow cytometric analysis (Fig. 4C) revealed that the cells expressing pBAD_AChy_700 (79% positive, mean = 251) were uniformly labeled when compared with pBAD_AM18_700 that expressed M18 scFv, which was uniformly negative (mean = 7). Furthermore, proteolytic activity of rChyB expressed from pBAD_AChy_700 could be inhibited by preincubation with 10 μ M soybean trypsin/chymotrypsin inhibitor (supplemental Fig. S7).

DISCUSSION

ATs comprise a large superfamily of extracellular virulence proteins secreted by Gram-negative bacteria (45). Despite the fact that the naturally occurring passengers of ATs exhibit diversity in sequence, function, and size, most of them do not contain widely spaced cysteines. This conserved feature has been reported to have resulted from structural constraints required for translocation across the outer membrane mediated by the C-terminal β -barrel. Since disulfide bonds are oxidized in the periplasm prior to translocation across the outer membrane, the export of native passenger variants containing widely spaced disulfides is severely restricted due to the aforementioned structural constraint (27). The inconsistencies in literature regarding the ability of ATs to export disulfide bond-containing passengers is further complicated by the fact that different studies use different ATs with different replacement points for the native or heterologous passengers. In this study, with the aid of quantitative flow cytometry, we have studied at

the single-cell level the ability of an *E. coli* AT Ag43 to export functional recombinant passenger molecules containing multiple disulfides by (a) varying the length of the native passenger by including/deleting the different domains comprising (i) the β -helical core, (ii) the autoproteolysis site, and (iii) the autochaperone domain containing the C-terminal β -hairpin and (b) varying the leader sequence that facilitates inner membrane translocation. As reported here, the efficient display of globular proteins such as the single-chain antibody fragment (two disulfides) against anthrax toxin or the serine protease chymotrypsin (four disulfides) can be accomplished in the absence of both the β -helical core (predicted aa 138–600 of Ag43) and the autochaperone domain (predicted aa 600–707 of Ag43). Based on our results, an intact β -barrel with the invariant α -helix is sufficient for the extracellular display of globular recombinant protein in a functional state. This is somewhat surprising given that slow folding of C-terminal region of passenger that folds into a β -helix has been implicated to be a crucial element for translocation/export (45, 46). Although it is likely that the globular structure of chymotrypsin is compatible with extracellular export via ATs given that the IgA protease (IgAP)/Hbp ATs contain a chymotrypsin/trypsin-like protease at their N terminus, two important distinctions need to be made (47, 48). First, the native IgAP/Hbp proteolytic components are located at the N terminus of the conserved β -helical core that is believed to facilitate their translocation whereas our recombinant construct, pBAD_AChy_700, displaying chymotrypsin is devoid of the β -helical passenger or the autochaperone domain. Second, the native passengers of IgAP/Hbp do not contain disulfide bonds, whereas rChyB is expected to contain four disulfide bonds, with one of the disulfide bonds bridging >50 aa (154–219, chymotrypsinogen numbering). These data suggest that our recombinant constructs might be similar in structure to *Pseudomonas aeruginosa* AT, EstA. The recently solved crystal structure of EstA indicated that unlike classical ATs, the esterase passenger of EstA adopts a globular structure dominated by α -helices and loops (49). Our results are consistent with the hypothesis that the requirement of the autochaperone domain is tied to the nature of the N-terminal passenger but is not a universal requirement. Similarly, the ability of Ag43 to translocate disulfide bond-containing proteins suggests that regardless of the spacing of the cysteines within the primary sequence, the overall globular structure of the passenger might dictate translocation efficiency, at least when heterologous proteins are being displayed. It remains to be tested whether other recombinant passengers that adopt a similar fold to single chain antibodies or chymotrypsin can be efficiently displayed using Ag43. The use of protease-deficient strains or reducing agents during protein expression did not have a positive effect on the surface display of recombinant proteins using the Ag43 system. In parallel, our data investigating the effect of the Sec-dependent extended N-terminal leader sequence indicated that genetic replacement with leader sequences of either outer membrane proteins or periplasmic proteins yielded display of functional passenger. In this regard, our data are consistent with a recent study indicating that the native signal peptide was not essential for either secretion or function of the plasmid-encoded toxin (Pet) AT (50).

AT-mediated Display of Proteins with Disulfide Bonds

It remains to be seen whether the modular architecture of Ag43 for heterologous display as demonstrated here is also applicable to other ATs. Our work also opens avenues for the engineering of recombinantly displayed proteins mediated by the Ag43 system comprising only the α -helix and the β -barrel by employing high-throughput flow cytometry (51, 52). A special feature of the AT extracellular transport system is that by including the autoproteolysis domain, switching between surface display and secretion of recombinant protein is rather straightforward (40).

Acknowledgments—We thank Drs. Leysath and Georgiou (University of Texas, Austin) for sharing resources/reagents. We also thank Dr. Goldberg (Massachusetts General Hospital) for providing *E. coli* MBG263. Microscopy experiments were performed at the laboratory of Dr. Golding (Baylor College of Medicine) with help from Leonardo A. Sepulveda. We also thank Dr. Conrad (University of Houston) for assistance with microscopy.

REFERENCES

- Schultheiss, E., Weiss, S., Winterer, E., Maas, R., Heinze, E., and Jose, J. (2008) Esterase autodisplay: enzyme engineering and whole-cell activity determination in microplates with pH sensors. *Appl. Environ. Microbiol.* **74**, 4782–4791
- Valls, M., Atrian, S., de Lorenzo, V., and Fernández, L. A. (2000) Engineering a mouse metallothionein on the cell surface of *Ralstonia eutropha* CH34 for immobilization of heavy metals in soil. *Nat. Biotechnol.* **18**, 661–665
- Li, C., Zhu, Y., Benz, I., Schmidt, M. A., Chen, W., Mulchandani, A., and Qiao, C. (2008) Presentation of functional organophosphorus hydrolase fusions on the surface of *Escherichia coli* by the AIDA-I autotransporter pathway. *Biotechnol. Bioeng.* **99**, 485–490
- Shibasaki, S., Ueda, M., Ye, K., Shimizu, K., Kamasawa, N., Osumi, M., and Tanaka, A. (2001) Creation of cell surface-engineered yeast that display different fluorescent proteins in response to the glucose concentration. *Appl. Microbiol. Biotechnol.* **57**, 528–533
- Binder, U., Matschiner, G., Theobald, I., and Skerra, A. (2010) High-throughput sorting of an Anticalin library via EspP-mediated functional display on the *Escherichia coli* cell surface. *J. Mol. Biol.* **400**, 783–802
- Jose, J., and Meyer, T. F. (2007) The autodisplay story, from discovery to biotechnical and biomedical applications. *Microbiol. Mol. Biol. Rev.* **71**, 600–619
- Nhan, N. T., Gonzalez de Valdivia, E., Gustavsson, M., Hai, T. N., and Larsson, G. (2011) Surface display of *Salmonella* epitopes in *Escherichia coli* and *Staphylococcus carnosus*. *Microb. Cell Fact.* **10**, 22
- Sander, L. E., Davis, M. J., Boeschoten, M. V., Amsen, D., Dascher, C. C., Ryffel, B., Swanson, J. A., Müller, M., and Blander, J. M. (2011) Detection of prokaryotic mRNA signifies microbial viability and promotes immunity. *Nature* **474**, 385–389
- Dautin, N., and Bernstein, H. D. (2007) Protein secretion in Gram-negative bacteria via the autotransporter pathway. *Annu. Rev. Microbiol.* **61**, 89–112
- Tseng, T. T., Tyler, B. M., and Setubal, J. C. (2009) Protein secretion systems in bacterial-host associations, and their description in the Gene Ontology. *BMC Microbiol.* **9**, S2
- Pallen, M. J., Chaudhuri, R. R., and Henderson, I. R. (2003) Genomic analysis of secretion systems. *Curr. Opin. Microbiol.* **6**, 519–527
- Henderson, I. R., Navarro-Garcia, F., Desvieux, M., Fernandez, R. C., and Ala'Aldeen, D. (2004) Type V Protein secretion pathway: the autotransporter story. *Microbiol. Mol. Biol. Rev.* **68**, 692–744
- Szabady, R. L., Peterson, J. H., Skillman, K. M., and Bernstein, H. D. (2005) An unusual signal peptide facilitates late steps in the biogenesis of a bacterial autotransporter. *Proc. Natl. Acad. Sci. U.S.A.* **102**, 221–226
- Wells, T. J., Tree, J. J., Ulett, G. C., and Schembri, M. A. (2007) Autotransporter proteins: novel targets at the bacterial cell surface. *FEMS Microbiol. Lett.* **274**, 163–172
- Rutherford, N., and Mourez, M. (2006) Surface display of proteins by Gram-negative bacterial autotransporters. *Microb. Cell Fact.* **5**, 22
- Pohlner, J., Halter, R., Beyreuther, K., and Meyer, T. F. (1987) Gene structure and extracellular secretion of *Neisseria gonorrhoeae* IgA protease. *Nature* **325**, 458–462
- Sauri, A., Soprova, Z., Wickström, D., de Gier, J. W., Van der Schors, R. C., Smit, A. B., Jong, W. S., and Luirink, J. (2009) The Bam (Omp85) complex is involved in secretion of the autotransporter haemoglobin protease. *Microbiology* **155**, 3982–3991
- Bernstein, H. D. (2007) Are bacterial 'autotransporters' really transporters? *Trends Microbiol.* **15**, 441–447
- Marin, E., Bodelón, G., and Fernández, L. A. (2010) Comparative analysis of the biochemical and functional properties of C-terminal domains of autotransporters. *J. Bacteriol.* **192**, 5588–5602
- Dautin, N., and Bernstein, H. D. (2011) Residues in a conserved α -helical segment are required for cleavage but not secretion of an *Escherichia coli* serine protease autotransporter passenger domain. *J. Bacteriol.* **193**, 3748–3756
- Oudega, B. (2003) *Protein Secretion Pathways in Bacteria*, pp. 111–113, Springer, The Netherlands
- Skillman, K. M., Barnard, T. J., Peterson, J. H., Ghirlando, R., and Bernstein, H. D. (2005) Efficient secretion of a folded protein domain by a monomeric bacterial autotransporter. *Mol. Microbiol.* **58**, 945–958
- Ieva, R., Skillman, K. M., and Bernstein, H. D. (2008) Incorporation of a polypeptide segment into the β -domain pore during the assembly of a bacterial autotransporter. *Mol. Microbiol.* **67**, 188–201
- Veiga, E., de Lorenzo, V., and Fernández, L. A. (2004) Structural tolerance of bacterial autotransporters for folded passenger protein domains. *Mol. Microbiol.* **52**, 1069–1080
- Brandon, L. D., and Goldberg, M. B. (2001) Periplasmic transit and disulfide bond formation of the autotransported *Shigella* protein IcsA. *J. Bacteriol.* **183**, 951–958
- Veiga, E., de Lorenzo, V., and Fernández, L. A. (1999) Probing secretion and translocation of a β -autotransporter using a reporter single-chain Fv as a cognate passenger domain. *Mol. Microbiol.* **33**, 1232–1243
- Leyton, D. L., Sevastyanovich, Y. R., Browning, D. F., Rossiter, A. E., Wells, T. J., Fitzpatrick, R. E., Overduin, M., Cunningham, A. F., and Henderson, I. R. (2011) Size and conformation limits to secretion of disulfide-bonded loops in autotransporter proteins. *J. Biol. Chem.* **286**, 42283–42291
- Jong, W. S., ten Hagen-Jongman, C. M., den Blaauwen, T., Slotboom, D. J., Tame, J. R., Wickström, D., de Gier, J. W., Otto, B. R., and Luirink, J. (2007) Limited tolerance towards folded elements during secretion of the autotransporter Hbp. *Mol. Microbiol.* **63**, 1524–1536
- Junker, M., Besingi, R. N., and Clark, P. L. (2009) Vectorial transport and folding of an autotransporter virulence protein during outer membrane secretion. *Mol. Microbiol.* **71**, 1323–1332
- Pyo, H. M., Kim, I. J., Kim, S. H., Kim, H. S., Cho, S. D., Cho, I. S., and Hyun, B. H. (2009) *Escherichia coli* expressing single-chain Fv on the cell surface as a potential prophylactic of porcine epidemic diarrhea virus. *Vaccine* **27**, 2030–2036
- Harvey, B. R., Georgiou, G., Hayhurst, A., Jeong, K. J., Iverson, B. L., and Rogers, G. K. (2004) Anchored periplasmic expression, a versatile technology for the isolation of high-affinity antibodies from *Escherichia coli*-expressed libraries. *Proc. Natl. Acad. Sci. U.S.A.* **101**, 9193–9198
- Vasquez, J. R., Evnin, L. B., Higaki, J. N., and Craik, C. S. (1989) An expression system for trypsin. *J. Cell. Biochem.* **39**, 265–276
- Jose, J., Krämer, J., Klausner, T., Pohlner, J., and Meyer, T. F. (1996) Absence of periplasmic DsbA oxidoreductase facilitates export of cysteine-containing passenger proteins to the *Escherichia coli* cell surface via the Iga β autotransporter pathway. *Gene* **178**, 107–110
- Varadarajan, N., Cantor, J. R., Georgiou, G., and Iverson, B. L. (2009) Construction and flow cytometric screening of targeted enzyme libraries. *Nat. Protoc.* **4**, 893–901
- Jeong, K. J., Seo, M. J., Iverson, B. L., and Georgiou, G. (2007) APEx 2-hybrid, a quantitative protein–protein interaction assay for antibody discov-

- ery and engineering. *Proc. Natl. Acad. Sci. U.S.A.* **104**, 8247–8252
36. Varadarajan, N., Gam, J., Olsen, M. J., Georgiou, G., and Iverson, B. L. (2005) Engineering of protease variants exhibiting high catalytic activity and exquisite substrate selectivity. *Proc. Natl. Acad. Sci. U.S.A.* **102**, 6855–6860
 37. Ausubel, F. M. (Ed) (1999) *Short Protocols in Molecular Biology: A Compendium of Methods from Current Protocols in Molecular Biology*, 4th Ed., pp. 10–48, Wiley, New York
 38. van der Woude, M. W., and Henderson, I. R. (2008) Regulation and function of Ag43 (flu). *Annu. Rev. Microbiol.* **62**, 153–169
 39. Kelley, L. A., and Sternberg, M. J. (2009) Protein structure prediction on the Web: a case study using the Phyre server. *Nat. Protoc.* **4**, 363–371
 40. Wargacki, A. J., Leonard, E., Win, M. N., Regitsky, D. D., Santos, C. N., Kim, P. B., Cooper, S. R., Raisner, R. M., Herman, A., and Sivitz, A. B. (2012) An engineered microbial platform for direct biofuel production from brown macroalgae. *Science* **335**, 308–313
 41. Voorhout, W. F., Leunissen-Bijvelt, J. J., Leunissen, J. L., and Verkleij, A. J. (1986) Steric hindrance in immunolabelling. *J. Microsc.* **141**, 303–310
 42. Leysath, C. E., Monzingo, A. F., Maynard, J. A., Barnett, J., Georgiou, G., Iverson, B. L., and Robertus, J. D. (2009) Crystal structure of the engineered neutralizing antibody M18 complexed to domain 4 of the anthrax protective antigen. *J. Mol. Biol.* **387**, 680–693
 43. Rutherford, N., Charbonneau, M. E., Berthiaume, F., Betton, J. M., and Mourez, M. (2006) The periplasmic folding of a cysteineless autotransporter passenger domain interferes with its outer membrane translocation. *J. Bacteriol.* **188**, 4111–4116
 44. Jose, J., and Zangen, D. (2005) Autodisplay of the protease inhibitor aprotinin in *Escherichia coli*. *Biochem. Biophys. Res. Commun.* **333**, 1218–1226
 45. Junker, M., Schuster, C. C., McDonnell, A. V., Sorg, K. A., Finn, M. C., Berger, B., and Clark, P. L. (2006) Pertactin β -helix folding mechanism suggests common themes for the secretion and folding of autotransporter proteins. *Proc. Natl. Acad. Sci. U.S.A.* **103**, 4918–4923
 46. Leyton, D. L., Rossiter, A. E., and Henderson, I. R. (2012) From self sufficiency to dependence: mechanisms and factors important for autotransporter biogenesis. *Nat. Rev. Microbiol.* **10**, 213–225
 47. Johnson, T. A., Qiu, J., Plaut, A. G., and Holyoak, T. (2009) Active-site gating regulates substrate selectivity in a chymotrypsin-like serine protease: the structure of *Haemophilus influenzae* immunoglobulin A1 protease. *J. Mol. Biol.* **389**, 559–574
 48. Otto, B. R., Sijbrandi, R., Luirink, J., Oudega, B., Heddle, J. G., Mizutani, K., Park, S. Y., and Tame, J. R. (2005) Crystal structure of hemoglobin protease, a heme binding autotransporter protein from pathogenic *Escherichia coli*. *J. Biol. Chem.* **280**, 17339–17345
 49. van den Berg, B. (2010) Crystal structure of a full-length autotransporter. *J. Mol. Biol.* **396**, 627–633
 50. Leyton, D. L., de Luna, M. G., Sevastyanovich, Y. R., Tveen Jensen, K., Browning, D. F., Scott-Tucker, A., and Henderson, I. R. (2010) The unusual extended signal peptide region is not required for secretion and function of an *Escherichia coli* autotransporter. *FEMS Microbiol. Lett.* **311**, 133–139
 51. Varadarajan, N., Rodriguez, S., Hwang, B. Y., Georgiou, G., and Iverson, B. L. (2008) Highly active and selective endopeptidases with programmed substrate specificities. *Nat. Chem. Biol.* **4**, 290–294
 52. Becker, S., Michalczyk, A., Wilhelm, S., Jaeger, K. E., and Kolmar, H. (2007) Ultrahigh-throughput screening to identify *E. coli* cells expressing functionally active enzymes on their surface. *ChemBioChem* **8**, 943–949
 53. Zeng, L., and Golding, I. (2011) Following cell-fate in *E. coli* after injection by phage lambda. *J. Vis. Exp.* **56**, 3363

Single-cell Characterization of Autotransporter-mediated *Escherichia coli* Surface Display of Disulfide Bond-containing Proteins

Balakrishnan Ramesh, Victor G Sendra, Patrick C Cirino and Navin Varadarajan

J. Biol. Chem. 2012, 287:38580-38589.

doi: 10.1074/jbc.M112.388199 originally published online September 27, 2012

Access the most updated version of this article at doi: [10.1074/jbc.M112.388199](https://doi.org/10.1074/jbc.M112.388199)

Alerts:

- [When this article is cited](#)
- [When a correction for this article is posted](#)

[Click here](#) to choose from all of JBC's e-mail alerts

Supplemental material:

<http://www.jbc.org/content/suppl/2012/09/27/M112.388199.DC1>

This article cites 51 references, 15 of which can be accessed free at

<http://www.jbc.org/content/287/46/38580.full.html#ref-list-1>